Journal of Alloys and Compounds 488 (2009) 380–385

Contents lists available at ScienceDirect

Journal of Alloys and Compounds

journal homepage: www.elsevier.com/locate/jallcom

Copper-substituted, lithium rich iron phosphate as cathode material for lithium secondary batteries

S.B. Lee [a], S.H. Cho [a], J.B. Heo [a], V. Aravindan [a], H.S. Kim [a,b], Y.S. Lee [a,*]

[a] Faculty of Applied Chemical Engineering, Chonnam National University, Gwang-ju 500-757, Republic of Korea
[b] Korea Electrotechnology Research Institute, 28-1 Seongju-dong, Changwon 641-120, Korea

ARTICLE INFO

Article history:
Received 15 July 2009
Accepted 30 August 2009
Available online 4 September 2009

Keywords:
Solid-state synthesis
$LiFePO_4$
$Li_{1.05}Fe_{0.997}Cu_{0.003}PO_4$
Rate capability
XPS

ABSTRACT

Carbon-free, copper-doped, lithium rich iron phosphates, $Li_{1+x}Fe_{1-y}Cu_yPO_4$ ($0 \le x \le 0.15$, $0 \le y \le 0.005$), have been synthesized by a solid-state reaction method. From the optimization, the $Li_{1.05}Fe_{0.997}Cu_{0.003}PO_4$ phase showed superior performances in terms of phase purity and high discharge capacity. The structural, morphological, and electrochemical properties were studied and compared to $LiFePO_4$, $Li_{1.05}FePO_4$, $LiFe_{0.997}Cu_{0.003}PO_4$, and materials. X-ray photoelectron spectroscopy (XPS) was conducted to ensure copper doping. Only smooth surface morphologies were observed for lithium rich iron phosphates, namely $Li_{1.05}FePO_4$ and $Li_{1.05}Fe_{0.997}Cu_{0.003}PO_4$. The $Li/Li_{1.05}Fe_{0.997}Cu_{0.003}PO_4$ cell delivered an initial discharge capacity of 145 mAh/g and was 18 mAh/g higher than the $Li/LiFePO_4$ cell without any carbon coating effect. Cyclic voltammetry revealed excellent reversibility of the $Li_{1.05}Fe_{0.997}Cu_{0.003}PO_4$ material. High rate capability studies were also performed and showed a capacity retention over 95% during the cycling. We concluded that substituted Li and Cu ions play an important role in enhancing battery performance of the $LiFePO_4$ material through improving the kinetics of the lithium insertion/extraction reaction on the electrode.

1. Introduction

Since the revolutionary work of Padhi et al. [1], polyanion-based olivine-type lithium iron phosphate ($LiFePO_4$) has become a target of increasing interest as a cathode material for lithium batteries from both an economic and environmental perspective. Iron is naturally more abundant, cost effective, and less toxic than other transition metals, especially in commercialized cells containing Co. Moreover, $LiFePO_4$ is found in nature as the mineral triphylite [2]. The $(PO_4)^{3-}$ polyanion itself provides structure stability and rises the redox energies ($Fe^{2+/3+}$) to levels exceeding those of layered oxides. In particular, the strong P–O covalent bond stabilizes the metal (Fe) anti-bonding state through an Fe–O–P inductive effect [3]. This effect not only offers an increase in cell potential, it also provides improved safety of the cell through strong P–O bonding [4]. The main obstacle that restricts the practical application of $LiFePO_4$ in lithium batteries is its poor rate capability, an aspect conventionally accepted as emanating primarily from its intrinsic electronic conductivity ($\sim 10^{-9}$ S/cm) [5].

Recently, extensive research has been directed at overcoming these issues by cationic doping, decreasing the particle size through solution-based synthesis, and coating with electronically conducting agents [3,5–10]. Recently, Kim et al. [11] reported the Li-deficient and Li-rich phases of Li_xFePO_4 ($x = 0.7$–1.1) that dramatically enhance the conducting properties of the material. An electronic conductivity between 10^{-3} and 10^{-1} S/cm was observed for both cases and six to seven orders of magnitude higher than the pure $LiFePO_4$ phase ($\sim 10^{-9}$ S/cm). Discharge capacities of 156 and 146 mAh/g were observed for Li-deficient and -rich phases, respectively. However, no cyclability has been reported and such phases contain impurities ranging from Li_3PO_4 to $Fe_2P_2O_7$. Interestingly, Croce et al. [12] reported the simple inclusion of Cu into the $LiFePO_4$ matrix, substantially improving the electrochemical performance of the cell with an observed discharge capacity >137 mAh/g. Ni et al. [13] also studied the Cu^{2+}-doped $LiFePO_4$ and achieved a discharge capacity of 141 mAh/g *via* co-precipitation, followed by ball milling. It is clear that incorporation of Cu into the $LiFePO_4$ lattice provided improved capacity either by addition or substitution, given the excellent conducting properties of copper. From previous reports, it is the conclusion of the authors that lithium or copper doping are quite effective in improving the electrical conductivity of $LiFePO_4$ material and can lead to remarkable improvements in the electrochemical performance of the $Li/LiFePO_4$ cell when two kinds of doping ions are used simultaneously during the synthetic process. In this context, for the first time, an attempt to optimize the synthesis of carbon-free, copper-doped, lithium rich iron phos-

* Corresponding author. Tel.: +82 62 530 1904; fax: +82 62 530 1909.
E-mail address: leeys@chonnam.ac.kr (Y.S. Lee).

0925-8388/$ – see front matter © 2009 Elsevier B.V. All rights reserved.
doi:10.1016/j.jallcom.2009.08.144

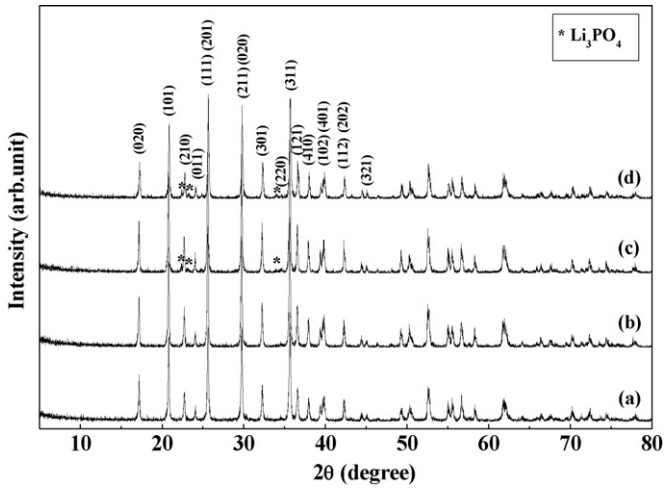

Fig. 1. XRD patterns of $Li_{1+x}FePO_4$ phase materials where x = (a) 0.00, (b) 0.05, (c) 0.10, and (d) 0.15.

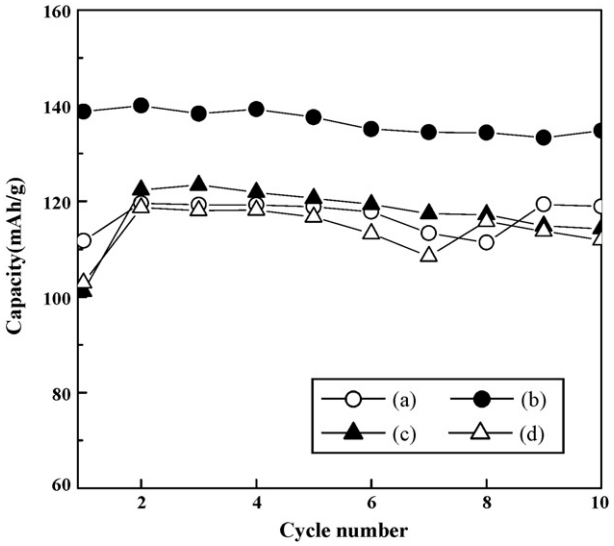

Fig. 2. Cycling profiles of $Li_{1+x}FePO_4$ phase materials where x = (a) 0.00, (b) 0.05, (c) 0.10, and (d) 0.15.

phates ($Li_{1+x}Fe_{1-y}Cu_yPO_4$ ($0 \le x \le 0.15$, $0 \le y \le 0.005$)) is made and the product compared with the parent $LiFePO_4$.

2. Experimental

Carbon-free, Cu-doped, lithium rich iron phosphate, $Li_{1+x}Fe_{1-y}Cu_yPO_4$ ($0 \le x \le 0.15$, $0 \le y \le 0.005$), materials were prepared by a conventional solid-state reaction method using the following source materials (Sigma–Aldrich, USA): Li_2CO_3; $FeC_2O_4{\cdot}2H_2O$; $(NH_4)_2HPO_4$; CuO. Stoichiometric ratios of the starting materials were finely ground using a mortar and calcined at 400 °C for 1.5 h for carbonate and oxalate decomposition. The product was again fine-ground and fired at 660 °C for 2.5 h under an Ar atmosphere to achieve the desired olivine phase. There is no carbon source or carbon coating treatment in order to improve electric conductivity, which can result in an unexpected effect to investigate improved cell property by small amount of Li and Cu doping.

X-ray diffraction (XRD, Rint 1000, Rigaku, Japan) studies were performed for structural analysis using Cu Kα radiation. Oxidation states of Fe and Cu in the structure were investigated by X-ray photoelectron spectroscopy (XPS, VG Inc. MultiLab 2000, UK). Each sample was measured after drying at 120 °C for 24 h. The source was monochromatic Al Kα radiation with a binding energy scan range of 1100–0 eV. The collected high-resolution XPS spectra were analyzed using an XPS peak-fitting program. The surface morphological features of the olivine-phased compounds were analyzed using a field emission scanning electron microscope (FE-SEM, S-4700, Hitachi, Japan). Electronic conductivity of the prepared material was studied through a conventional four probe apparatus (Keithley Instruments, 2182A, USA). Cyclic voltammetry (CV) was performed using a Solartron (1287, Ameteck, UK) with a three-electrode cell configuration. In the CV measurements, the Li metal served as a counter and reference electrode in a voltage range of 2.5–4.2 V, at a 0.02 mV/s scanning rate. Cycling performances were performed using a CR2032 coin-type cell between 2.8 and 4.0 V at room temperature. The composite cathode was fabricated with 20.0 mg of accurately weighed active material, 3.0 mg of Ketzen black (KB), and 3.0 mg of conductive binder (2.0 mg of Teflonized acetylene black (TAB) and 1.0 mg of graphite). This was then pressed on a 200-mm^2 stainless steel mesh that served as the current collector under a pressure of 300 kg/cm^2 and was dried at 130 °C for 5 h in an oven. The cell was composed of a cathode and a metallic lithium anode separated by a porous polypropylene film (Celgard 3401). A 1.0 M $LiPF_6$ in ethylene carbonate (EC):dimethyl carbonate (DMC) (1:1, v/v, Techno Semichem Co., Ltd, Korea) mixture was used as the electrolyte.

3. Results and discussion

It is well known that variations in the stoichiometric proportions of the Li content lead to drastic improvements in the conducting behavior of olivine phase materials [11,14–16]. At the same time, however, structural properties cannot be ruled out. Thus, meticulous care has been taken towards optimization of Li inclusion in the pure phase. Optimization of the Li content in the $Li_{1+x}FePO_4$ lattice was performed based on the phase purity, as well as discharge capacity. Concentration of the Li content was varied according to composition ($0 \le x \le 0.15$) *viz*, 0.00, 0.05, 0.10, and 0.15. Powder XRD was utilized to analyze the structural properties of the $Li_{1+x}FePO_4$ phase materials, Fig. 1. It is evident that a small amount of (0.05) Li addition in the $LiFePO_4$ matrix did not prompt any structural deformation. However, if the Li content exceeded 0.05, it lead to formation of an impurity phase, such as Li_3PO_4, confirmed by bands at $2\theta = 22.4$, 23.3, and 33.9°. These impurity phases are consistent with the previous reports on stoichiometric variations in Li content [11,14]. Furthermore, it is held that the presence of Li_3PO_4 may affect the electrochemical performance of the cell. Thus, in order to corroborate this, a cycling study was performed for all olivine rich materials prepared and is presented in Fig. 2. The cycling studies of the $Li_{1+x}FePO_4$ ($0 \le x \le 0.15$) phase were carried out between the cut-off limits of 2.8 and 4.0 V at room temperature. It is apparent that nearly all the materials showed that same capacity at ~120 mAh/g, except the $Li_{1.05}FePO_4$ phase (139 mAh/g). From this, it may be inferred that the inferior conductivity of the $LiFePO_4$, and the rest of the phases, suffered due to the presence of Li_3PO_4 moieties, and as such, offered much diminished performances. It is to conclude that, Li content of 0.05 is optimum concentration along with stoichiometric ratio to search for the lithium rich iron phosphates in terms of its purity and capacity profile in this study.

Similarly, cationic substitution is a unique approach to improve discharge capacities in $LiFePO_4$-based materials [5,6,9,10]. Copper substitution was made for the Fe sites in the $Li_{1.05}Fe_{1-y}Cu_yPO_4$ ($0 \le y \le 0.005$) phase to further extend its capacity profile. Structural profiles of the $Li_{1.05}Fe_{1-y}Cu_yPO_4$ phases were recorded using powder X-ray diffractometry as shown in Fig. 3. The obtained XRD patterns were also compared to $LiFePO_4$ and are presented. From these, no appreciable change is noticeable. This may be a result of the concentration of the doping substance being too small and as such, is very hard to detect through XRD due to the instrumental standards. Further, all the prepared materials exhibited crystallized well and without the presence of impurities, such as like Li_3PO_4 (as observed during the optimization of Li-rich content).

With the intention of studying the effects of copper substitution in $Li_{1.05}Fe_{1-y}Cu_yPO_4$ ($0 \le y \le 0.005$) materials, galvanostatic charge/discharge studies were performed and shown in Fig. 4. Initial discharge capacities of 103, 110, 145, 139, and 120 mAh/g were observed for cells comprised of various $Li_{1.05}Fe_{1-y}Cu_yPO_4$ samples, where y = 0.001, 0.002, 0.003, 0.004, and 0.005, respectively. As shown in Fig. 4, the Li/$Li_{1.05}Fe_{0.997}Cu_{0.003}PO_4$ cell exhibited superior performance among the concentrations studied. It can be noted that increasing Cu substitution leads to an increase in the capacity

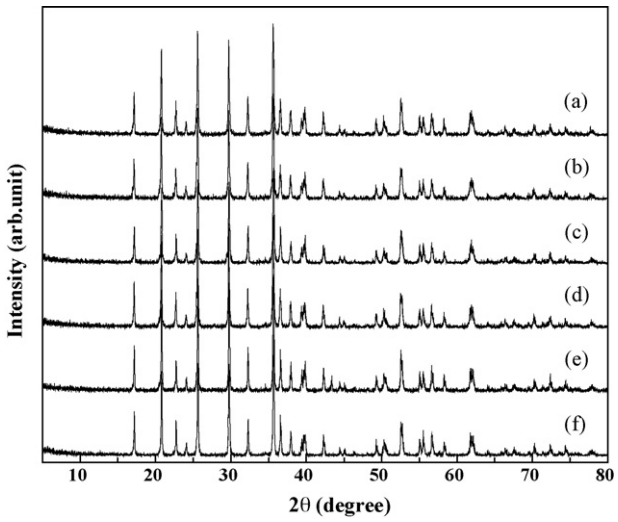

Fig. 3. XRD patterns of $Li_{1.05}Fe_{1-y}Cu_yPO_4$ phase materials where y = (a) 0.001, (b) 0.002, (c) 0.003, (d) 0.004, and (e) 0.005.

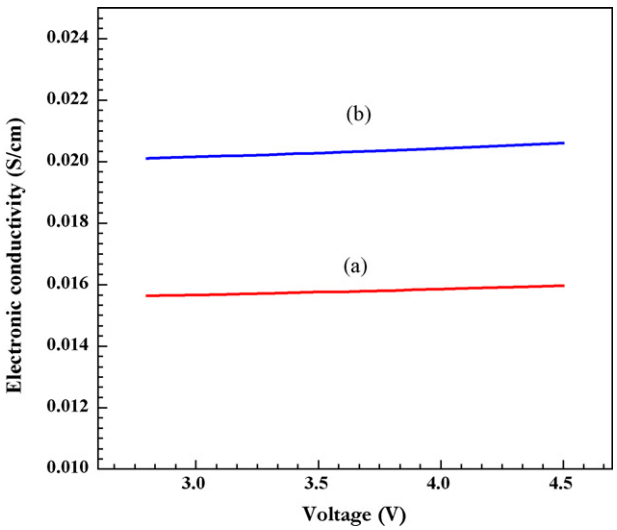

Fig. 5. Electronic conductivity profiles of (a) $Li_{1.05}FePO_4$ and (b) $Li_{1.05}Fe_{0.997}Cu_{0.003}PO_4$.

profile. The substitution of Cu exceeded the concentration level of 0.003 and lead to capacity fading of the cell. A similar kind of variation in the capacity profile was observed by Wu et al. [17] and Nakamura et al. [18] for Ti^{4+} and Mn^{2+} substitution, respectively, for Fe sites.

There are two arguments regarding the origin of such improvements in capacity profiling. Capacity improvements achieved by increasing conducting properties of the host lattice are known. The first argument suggests that the doping effect, as a relevant influence on conductivity, increases through modification of the electronic structure of $LiFePO_4$ [19]. The second argument involves a low-valency iron derivative as responsible for the high conductivity in these compounds rather than the doping effect [20]. Resolution of this controversial issue is not paramount, and the exact mechanism for such improvement is a heated topic of research in $LiFePO_4$ cathodes [5,21]. In order to crosscheck the aforementioned arguments, the electronic conductivity of the prepared materials was measured as a function of applied voltage. The specimen used for the conductivity measurement was composed of 20.0 mg of active material, 0.3 mg of KB, and 0.3 mg TAB. Fig. 5 clearly indicates that the Li-rich phase, $Li_{1.05}FePO_4$, exhibited conductivity on the order of $\sim 10^{-2}$ S/cm at room temperature. This result corroborates a previous report by Kim et al. [11]. Moreover, substitution of copper for Fe^{2+} sites substantially improved the conducting properties of the olivine phase in addition to favoring the argument by Abbate et al. [19].

In order to more clearly investigate lithium and copper doping effects in $LiFePO_4$, the $LiFe_{0.997}Cu_{0.003}PO_4$ material was also prepared and compared with other optimized materials, along with its pure phase. The X-ray diffraction measurements were performed and compared with $LiFePO_4$ and various olivine materials. Fig. 6 shows that the XRD pattern suggests the existence of an orthorhombic structure with a *Pnma* space group for all prepared materials. In addition, it clearly shows the absence of impurity phases like FeP, Fe_2P, Li_3PO_4, and $Fe_2P_2O_7$ [11,14]. These impurities may form from improper synthetic conditions, as well as Li contents higher ($Li_{>1.05}FePO_4$) or lower ($Li_{<0.96}FePO_4$) than particular levels in the stoichiometric phase [11,14]. In order to ascertain the phase purity of the material synthesized, the lattice parameters were calculated and tabulated (Table 1). The observed lattice constants are in close proximity with previously reported values [11,22] and confirm the excellent phase purity of the materials.

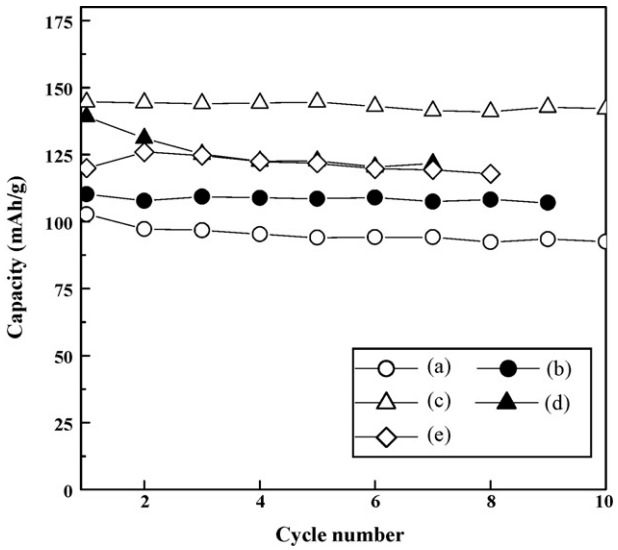

Fig. 4. Cycling profiles of $Li_{1.05}Fe_{1-y}Cu_yPO_4$ phase materials where y = (a) 0.001, (b) 0.002, (c) 0.003, (d) 0.004, and (e) 0.005.

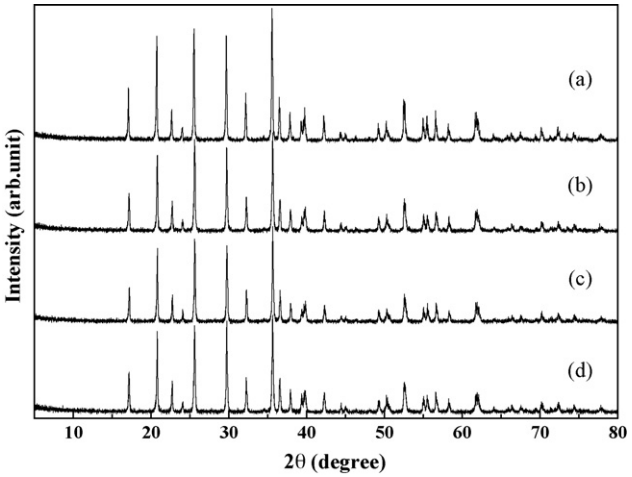

Fig. 6. XRD patterns of (a) $LiFePO_4$, (b) $Li_{1.05}FePO_4$, (c) $LiFe_{0.997}Cu_{0.003}PO_4$, and (d) $Li_{1.05}Fe_{0.997}Cu_{0.003}PO_4$.

Table 1
Powder properties of olivine phase materials prepared by solid-state synthesis.

Sample	a (Å)	b (Å)	c (Å)	α (°)	β (°)	γ (°)	V (Å)^3
$LiFePO_4$	10.347	6.019	4.699	90	90	90	2.926
$Li_{1.05}FePO_4$	10.335	6.011	4.699	90	90	90	2.921
$LiFe_{0.997}Cu_{0.003}PO_4$	10.331	6.012	4.698	90	90	90	2.920
$Li_{1.05}Fe_{0.997}Cu_{0.003}PO_4$	10.323	6.006	4.692	90	90	90	2.918

Presence of the Cu ion in the $Li_{1.05}Fe_{0.997}Cu_{0.003}PO_4$ phase was analyzed by X-ray photoelectron spectroscopy (XPS). The XPS spectra was obtained by irradiating the sample with a beam of X-rays while simultaneously measuring the kinetic energy (in eV) and number of electrons escaping from the top 1–10 nm of the material being analyzed. This technique is well suited for battery applications, particularly in the evaluation of the valance states of the metal/non-metal used in cathodes and anodes and the interfacial studies between the components [23,24]. The core level spectra of $Li_{1.05}Fe_{0.997}Cu_{0.003}PO_4$ are shown in Fig. 7. The C 1 shown at 284.5 eV indicates the presence of carbon [25]. The presence (or trace amount) of carbon is unavoidable when using organic salt-based starting materials [14]. The O 1s and P 2p demonstrated their presence at 531.48 and 133.49 eV, respectively, and belong to the phosphate moiety. The absence of overlapping bands in the core level of the P 2p suggests a phase purity of the material, the absence of Li_3PO_4 [26]. Multiple splitting energy levels of the Fe ion give rise to two satellite bands at 711.13 eV ($2p_{3/2}$) and 724.49 eV ($2p_{1/2}$) and confirm the triphylite phase [23,26]. The Li 1s showed a binding energy at 55.50 eV, which is in good agreement with earlier reports [26]. It is well known that the appearance of the spin–orbit

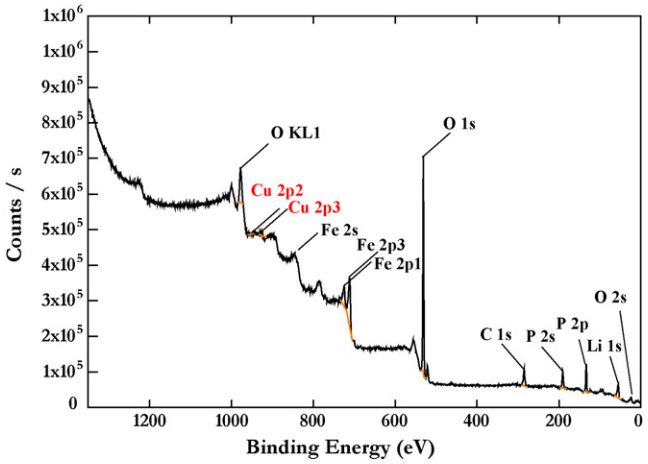

Fig. 7. X-ray photoelectron spectroscopic (XPS) traces of $Li_{1.05}Fe_{0.997}Cu_{0.003}PO_4$.

splitting of Cu ($2P_{3/2}$ 931.18 eV and $2P_{1/2}$ 952.48 eV), along with their vibrate up satellites, is mainly a feature of divalent copper. Apparently, such spectra showed two satellite peaks at reduced intensities, representing the existence of Cu^{2+} [27].

Fig. 8 presents the surface morphologies of the different olivine materials synthesized by the solid-state method. It is readily apparent that smooth and well-defined particulates were observed for lithium rich phases, such as $Li_{1.05}FePO_4$ (Fig. 7(b)) and $Li_{1.05}Fe_{0.997}Cu_{0.003}PO_4$ (Fig. 7(d)), whereas the rest of the materials bear rough surface morphologies. $LiFePO_4$ and $LiFe_{0.997}Cu_{0.003}PO_4$

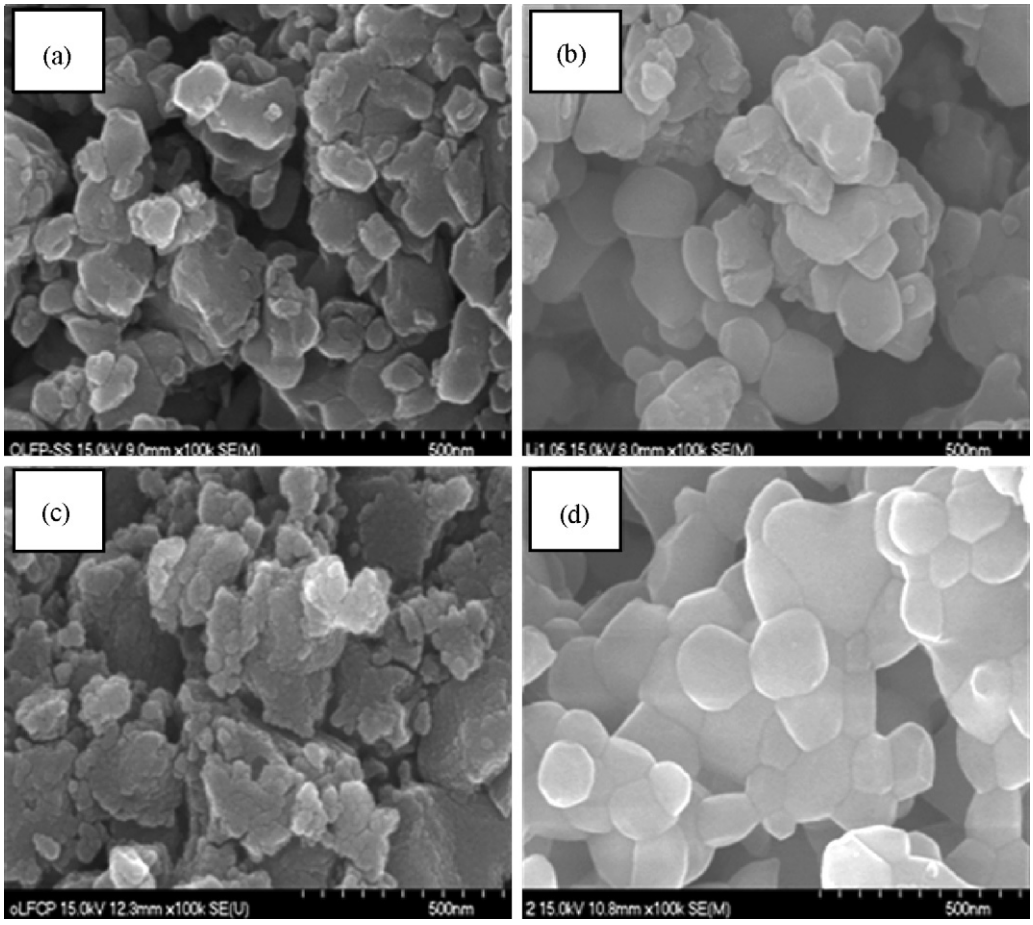

Fig. 8. SEM images of (a) $LiFePO_4$, (b) $Li_{1.05}FePO_4$, (c) $LiFe_{0.997}Cu_{0.003}PO_4$, and (d) $Li_{1.05}Fe_{0.997}Cu_{0.003}PO_4$.

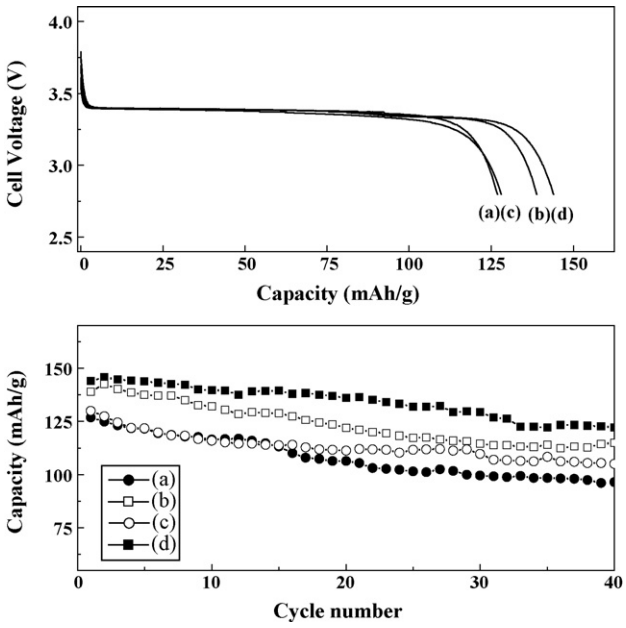

Fig. 9. Initial discharge curves and cycling performances of Li/(a) $LiFePO_4$, (b) $Li_{1.05}FePO_4$, (c) $LiFe_{0.997}Cu_{0.003}PO_4$, and (d) $Li_{1.05}Fe_{0.997}Cu_{0.003}PO_4$ cells.

were composed of many large polycrystalline type particles ranging from 100 to 200 nm, and small particles from 20 to 50 nm distributed among the larger particles. Each particle was completely separated and located without any linkage. However, $Li_{1.05}FePO_4$ and $Li_{1.05}Fe_{0.997}Cu_{0.003}PO_4$ showed a slightly increased particle size and different particle morphology from the other two materials. In particular, the surface morphology of $Li_{1.05}Fe_{0.997}Cu_{0.003}PO_4$ seemed to melt and combine together during the synthetic process, connecting with each other to form micrometer size lumps. It is the suggestion of the authors that a small amount of Li or Li and Cu double substitution in the $LiFePO_4$ changes its structural properties and particle morphology, enhances the contact area between the particles, and improves electrical conductivity of the electrode, although only partially in this material [28].

Fig. 9 represents the first discharge curves of the four olivine materials, comparing and corresponding cycling profiles. All four materials showed a concrete flat voltage region at 3.4 V, although there was a sizable difference in discharge capacity. These cells delivered initial discharge capacities of 127, 128, 139, and 145 mAh/g for $LiFePO_4$, $LiFe_{0.997}Cu_{0.003}PO_4$, $Li_{1.05}FePO_4$, and $Li_{1.05}Fe_{0.997}Cu_{0.003}PO_4$ at room temperature, respectively. Substitution of copper into pure $LiFePO_4$ lead to a negligible amount of capacity improvement in the first cycle. However, it experienced improved stability over $LiFePO_4$ during prolonged cycling. This result confirms the doping of Cu into the olivine phase for capacity enhancement *via* the improved electronic conductivity and is analogous to the earlier report related to Cu inclusion/substitution [12,13]. Nevertheless, lithium rich olivine material ($Li_{1.05}FePO_4$) containing cells only exhibited a discharge capacity of 139 mAh/g, a higher value (12 mAh/g) than pristine $LiFePO_4$ material. This may be attributed to the increased electronic conductivity of the material through addition of excess lithium ions. In order to further improve discharge capacities in $LiFePO_4$ materials, $Li_{1.05}Fe_{0.997}Cu_{0.003}PO_4$ results in an enhanced capacity of 145 mAh/g without carbon coating. The specific discharge capacities *versus* cycle number for four materials are shown in Fig. 9. As expected, the cell comprising the $Li_{1.05}Fe_{0.997}Cu_{0.003}PO_4$ phase exhibited performance superior to other materials. The cell experienced a capacity retention of over 85% at the end of the 40th cycle, whereas only 76% retention was observed for the pure $LiFePO_4$. This level of improved retention

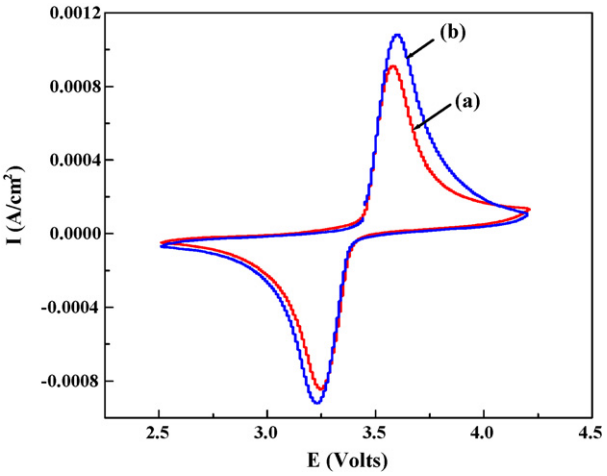

Fig. 10. Cyclic voltammograms (CV) of (a) $LiFePO_4$ and (b) $Li_{1.05}Fe_{0.997}Cu_{0.003}PO_4$.

may be attributed to the inclusion of more lithium (lithium rich phase) as well as the substitution of copper. As a result, the conductivity enhancement of the cathode material with compositional modifications confirms the conductivity improvement of the cathode, which is important for its practical use in lithium secondary batteries.

The cyclic voltammogram (CV) of the $LiFePO_4$ and $Li_{1.05}Fe_{0.997}Cu_{0.003}PO_4$ are shown in Fig. 10. The materials exhibited sharp oxidation (~3.5 V) and reduction (~3.3 V) peaks, reliable with a two-phase reaction at ~3.4 V *versus* Li^+/Li. No other peaks were observed, indicating the absence of electroactive iron impurities. The well-defined peak and symmetrical form of the CV traces explain the outstanding reversibility of the lithium extraction/insertion reactions in the prepared materials. Notably, the increased cathodic and anodic current values of $Li_{1.05}Fe_{0.997}Cu_{0.003}PO_4$ represent well the improved kinetic properties of such a phase during the redox process [23,29,30].

Rate capability studies were also performed for $Li/LiFePO_4$ and $Li/Li_{1.05}Fe_{0.997}Cu_{0.003}PO_4$ cells as presented in Fig. 11. Different current densities from 0.5 to 3 C have been employed at room temperature. At 0.5 C, the $LiFePO_4$ and $Li_{1.05}Fe_{0.997}Cu_{0.003}PO_4$ materials exhibited discharge capacities of 83 and 120 mAh/g, respectively. The current densities were subsequently increased to 3 C with

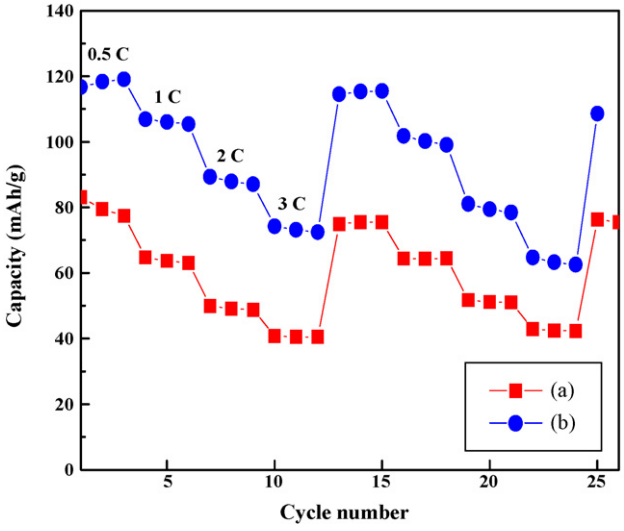

Fig. 11. Rate capability performances of Li/(a) $LiFePO_4$ and (b) $Li_{1.05}Fe_{0.997}Cu_{0.003}PO_4$ cells at room temperature.

discharge capacities of 41 and 75 mAh/g obtained for $LiFePO_4$ and $Li_{1.05}Fe_{0.997}Cu_{0.003}PO_4$ materials. These rare capability studies were repeated as a cycle and exhibited an over 95% retention in capacity at higher current rates for $Li_{1.05}Fe_{0.997}Cu_{0.003}PO_4$. Based on these results, it is the recommendation of the authors that the substituted Li and Cu ions play an important role in enhancing battery performance of the $LiFePO_4$ material through improving the kinetics of the lithium oxidation/reduction reaction on the electrode by enlarging the contact area of the particles. Moreover, the $Li_{1.05}Fe_{0.997}Cu_{0.003}PO_4$ material can be prepared very easily without any further post-treatments like carbon coating or ball milling, routes suggested by several authors to improve the battery performance of olivine structured material [3,5,9,10].

4. Conclusions

Carbon-free, copper-doped, lithium rich olivine phosphate material ($Li_{1+x}Fe_{1-y}Cu_yPO_4$ ($0 \le x \le 0.15$, $0 \le y \le 0.005$)) was prepared by a solid-state reaction method under an Ar atmosphere at 660 °C. The $Li_{1.05}Fe_{0.997}Cu_{0.003}PO_4$ phase exhibited superior cell performance among the materials prepared. Phase purity and powder properties were investigated by XRD analysis. The Cu substitution was confirmed by XPS measurements, which improved the conducting properties of the olivine phase. The $Li/Li_{1.05}Fe_{0.997}Cu_{0.003}PO_4$ cell showed an initial discharge capacity of 145 mAh/g and was 18 mAh/g higher than pristine $LiFePO_4$ at room temperature. Rate performance studies also demonstrated the high rate capabilities of the prepared material to reveal a >95% capacity retention over the investigated cycling.

Acknowledgements

This work was supported by a grant (Code#: 2009K000446) from the 'Center for Nanostructured Materials Technology', under the '21st Century Frontier R & D programs' of the Ministry of Education, Science and Technology, Korea.

References

[1] A.K. Padhi, K.S. Nanjundaswamy, J.B. Goodenough, J. Electrochem. Soc. 144 (1997) 1188–1194.
[2] M. Koltypin, D. Aurbach, L. Nazar, B. Ellis, J. Power Sources 174 (2007) 1241–1250.
[3] A. Manthiram, A.V. Murugan, A. Sarkar, T. Muraliganth, Energy Environ. Sci. 1 (2008) 621–638.
[4] J. Cho, Y.W. Kim, B. Kim, J.G. Lee, B. Park, Angew. Chem. Int. Ed. 42 (2003) 1618–1621.
[5] Z. Li, D. Zhang, F. Yang, J. Mater. Sci. 44 (2009) 2435–2443.
[6] S.Y. Chung, J.T. Bloking, Y.M. Chiang, Nat. Mater. 1 (2002) 123–128.
[7] K.S. Park, S.B. Schougaard, J.B. Goodenough, Adv. Mater. 19 (2007) 848–851.
[8] B. Ellis, W.H. Kan, W.R.M. Makahnouk, L.F. Nazar, J. Mater. Chem. 17 (2007) 3248–3254.
[9] D. Jugovic, D. Uskokovic, J. Power Sources 190 (2009) 538–544.
[10] C. Gouri, Lithium Iron Phosphate—A Promising Cathode-Active Material for Lithium Secondary Batteries, Trans Tech Publishers, 2008.
[11] D.K. Kim, H.M. Park, S.J. Jung, Y.U. Jeong, J.H. Lee, J.J. Kim, J. Power Sources 159 (2006) 237–240.
[12] F. Croce, A. D'Epifanio, J. Hassoun, A. Deptula, T. Olczac, B. Scrosati, Electrochem. Solid State Lett. 5 (2002) A47–A50.
[13] J.F. Ni, H.H. Zhou, J.T. Chen, X.X. Zhang, Mater. Lett. 59 (2005) 2361–2365.
[14] P.S. Herle, B. Ellis, N. Coombs, L.F. Nazar, Nat. Mater. 3 (2004) 147–152.
[15] S. Shi, L. Liu, C. Ouyang, D.S. Wang, Z. Wang, L. Chen, X. Huang, Phys. Rev. B 68 (2003) 195108-1–195108-5.
[16] P.G. Bruce, B. Scrosati, J.M. Tarascon, Angew. Chem. Int. Ed. 47 (2008) 2930–2946.
[17] S.H. Wu, M.S. Chen, C.J. Chien, Y.P. Fu, J. Power Sources 189 (2009) 440–444.
[18] T. Nakamura, Y. Miwa, M. Tabuchi, Y. Yamada, J. Electrochem. Soc. 153 (2006) A1108–A1114.
[19] M. Abbate, S.M. Lala, L.A. Montoro, J.M. Rosolen, Electrochem. Solid State Lett. 8 (2005) A288–A290.
[20] N. Ravet, A. Abouimrane, M. Armand, Nat. Mater. 2 (2003) 702–1702.
[21] V. Lemos, S. Guerini, J.M. Filho, S.M. Lala, L.A. Montoro, J.M. Rosolen, Solid State Ionics 177 (2006) 1021–1025.
[22] S.T. Myung, S. Komaba, N. Hirosaki, H. Yashiro, N. Kumagai, Electrochim. Acta 49 (2004) 4213–4222.
[23] K. Saravanan, M.V. Reddy, P. Balaya, H. Gong, B.V.R. Chowdari, J.J. Vittal, J. Mater. Chem. 19 (2009) 605–610.
[24] S.K. Martha, B. Markovsky, J. Grinblat, Y. Gofer, O. Haik, E. Zinigrad, D. Aurbach, T. Drezen, D. Wang, G. Deghenghi, I. Exnar, J. Electrochem. Soc. 156 (2009) A541–A552.
[25] M. Herstedt, M. Stjerndahl, A. Nyten, T. Gustafsson, H. Rensmo, H. Siegbahn, N. Ravet, M. Armand, J.O. Thomas, K. Edström, Electrochem. Solid State Lett. 6 (2003) A202–A206.
[26] Y.H. Rho, L.F. Nazar, L. Perry, D. Ryan, J. Electrochem. Soc. 154 (2007) A283–A289.
[27] J.P. Espinos, J. Morales, A. Barranco, A. Caballero, J.P. Holgado, A.R.G. Elipe, J. Phys. Chem. B 106 (2002) 6921–6929.
[28] X. Luo, X. Wang, L. Liao, S. Gamboa, P.J. Sebastian, J. Power Sources 158 (2006) 654–658.
[29] V. Palomares, A. Goñi, I.G.D. Muro, I.D. Meatza, M. Bengoechea, O. Miguel, T. Rojo, J. Power Sources 171 (2007) 879–885.
[30] J.B. Heo, S.B. Lee, S.H. Cho, J. Kim, S.H. Park, Y.S. Lee, Mater. Lett. 63 (2009) 581–583.